Accelerometry-Based Estimation of Respiratory Rate for Post-Intensive Care Patient Monitoring

Delaram Jarchi, Sarah J. Rodgers, Lionel Tarassenko, and David A. Clifton

***Abstract*— This paper evaluates the use of accelerometers for continuous monitoring of respiratory rate (RR), which is an important vital sign in post-intensive care patients or those inside the intensive care unit (ICU). The respiratory rate can be estimated from accelerometer and photoplethysmography (PPG) signals for patients following ICU discharge. Due to sensor faults, sensor detachment, and various artifacts arising from motion, RR estimates derived from accelerometry and PPG may not be sufficiently reliable for use with existing algorithms. This paper described a case study of 10 selected patients, for which fewer RR estimates have been obtained from PPG signals in comparison to those from accelerometry. We describe an algorithm for which we show a maximum mean absolute error between estimates derived from PPG and accelerometer of 2.56 breaths/min. Our results obtained using the 10 selected patients are highly promising for estimation of RR from accelerometers, where significant agreements have been observed with the PPG-based RR estimates in many segments and across various patients. We present this research as a step towards producing reliable RR monitoring systems using low-cost mobile accelerometers for monitoring patients inside the ICU or on the ward (post-ICU).**

***Index Terms*— Respiratory rate (RR), accelerometer, photoplethysmography (PPG), adaptive line enhancer (ALE), auto-regressive (AR).**

I. Introduction

INTELLIGENT monitoring of vital signs (such as heart rate, respiratory rate (RR), blood oxygen saturation level (SpO2) and blood pressure) in unobtrusive ways is crucial to transform recognition of patients at risk of deterioration. Replacement of manual recordings of physiological parameters through the nurses (which are not always accurate or repeatable) was considered as a priority to improve healthcare systems [1].

The respiratory rate is measured in the hospitals from manual counting of the breaths as the simplest form, conventional impedance pneumography (IP) or an optical technique called end-tidal carbon dioxide (et-CO2). The IP based method as a noninvasive method to estimate RR is highly susceptible to motion and posture changes of the subject [2] and it is very likely to produce erroneous results [3]. In the IP-based method, injection of a low-amplitude high-frequency current into the thorax at ECG electrodes has been performed to measure variations in thoracic impedance. This output impedance has a strong correlation with respiration [4]. In the method using et-CO2, a device called capnometer that uses a small plastic tube is inserted inside the patient's mouth. The tube of the capnometer accumulates expelled CO2 in each breath. The infrared radiation, then, emits a light source that moves through the CO2. Following absorption of infrared radiation over time, a variation with breathing rate will be induced. The et-CO2 based systems are used in the hospitals mainly for patients in critical care. For continuous monitoring of RR in clinical environment, both IP and et-CO2 methods suffer from limitations in terms of patient compliance and accuracy. These limitations also affect validation of any respiratory based monitory system. Portable or wearable systems could suffer from more limitations but they are less obtrusive and therefore good candidates for long-term monitoring of the patients including an increased patient compliance. Therefore, the main challenge in the use of portable/wearable systems will be finding ways to improve the accuracy of the designed respiratory rate monitoring system.

Advanced technology introduced wearable sensors which have been evaluated in many studies to enable automatic and accurate estimation of vital signs. Respiratory rate has been investigated the least in research studies compared to e.g. heart rate, which has been extensively under analysis for continuous improvements of the corresponding developed algorithms. Respiratory rate is a key physiological measurement in patient care systems used to quantify risk of patient deterioration [5] [6]. It has been reported in previous studies that abnormal respiratory rate is a highly informative indicator of adverse events such as clinical deterioration [7]–[10] and [11]. Photoplethysmography (PPG) based estimation of respiratory rate has been proposed in recent studies [12]–[14]. A comprehensive review of PPG and electrocardiography (ECG) based algorithms for respiratory rate based estimation has been conducted in [15]. There are other research studies with interests on the use of contact-free systems to estimate respiratory rate. These include the use of thermal and depth imaging camera video [16], a multimodal system containing pyro-electric infrared and vibration sensors [17] and video images to monitor respiration in the neonatal intensive care unit [18].

Acceleration signals have been used for many motion analysis applications such as gait, posture, and balance analysis. The use of accelerometers for motion analysis has significantly increased due to their ease of use, portability, and ability to be integrated in low-power wireless embedded platforms. The aim of this research is to investigate the use of accelerometers to estimate RR in clinical environments. Two methods are

Manuscript received March 1, 2018; revised April 5, 2018; accepted April 5, 2018. Date of publication April 19, 2018; date of current version May 22, 2018. This work was supported by the U.K. Engineering and Physical Sciences Research Council under Grant EP/N024966/1. The associate editor coordinating the review of this paper and approving it for publication was Dr. Edward Sazonov. *(Corresponding author: Delaram Jarchi.)*

The authors are with the Department of Engineering Science, University of Oxford, Oxford OX3 7DQ, U.K. (e-mail: delaram.jarchi@eng.ox.ac.uk; sarah-jane.rodgers@balliol.ox.ac.uk; lionel.tarassenko@eng.ox.ac.uk; davidc@robots.ox.ac.uk).

Digital Object Identifier 10.1109/JSEN.2018.2828599

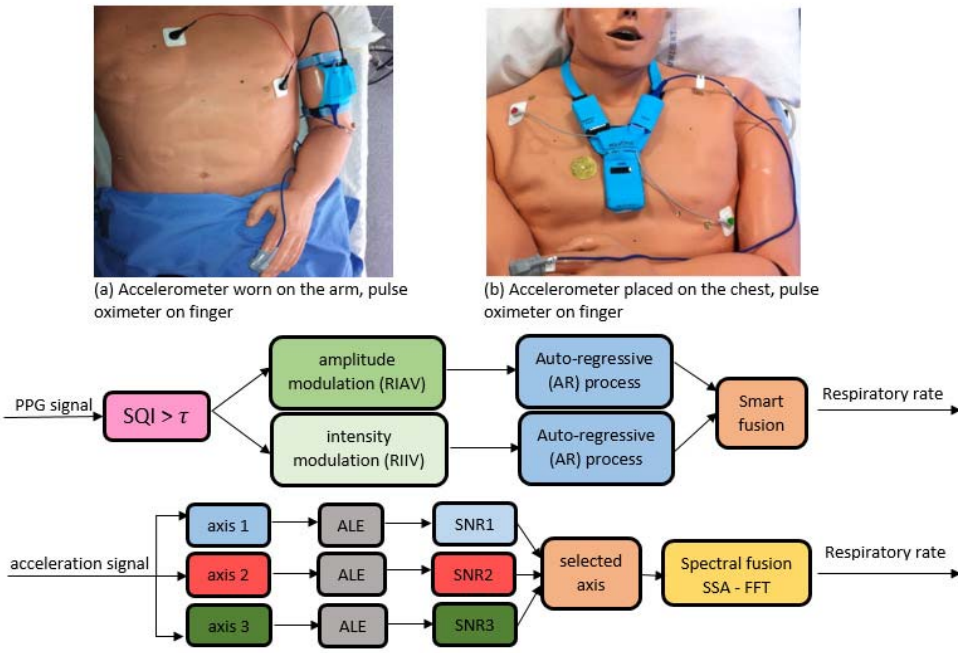

Fig. 1. The wearable sensors including ECG, PPG, and accelerometers are shown. For some of the patients, an arm worn accelerometer has been used while for other patients the accelerometer was placed on the chest. The arm worn sensor is specifically useful for patients who have upper gastrointestinal surgery. The block digram of the algorithmic stages to estimate RR from input PPG signal (*top row*) and acceleration signal (*bottom row*) are also shown in this figure.

proposed to estimate RR from PPG and accelerometer. The core of the PPG method is based on a recent research proposed in [14]. For the acceleration method, various signal processing techniques are combined to produce an estimate of respiratory rate. The accelerometry-based estimates of RR are compared to the PPG-based estimates. The results obtained for patients discharged from intensive care unit (ICU) demonstrate significant agreements between acceleration- and PPG-based estimates of RR. This research is a big step toward continuous monitoring of respiratory rate using accelerometers for monitoring of ICU patients.

The remainder of the paper is organised as follows. In Section II, first, the recorded dataset has been explained. Then, PPG-based algorithm for estimation of respiratory rate has been provided. This has been followed by introducing the accelerometer based algorithm to estimate RR. The experimental results are provided in Section III. Finally, Section IV concludes the paper by highlighting the significance of the results, potential improvements and future work.

II. Materials and Methods

A. Dataset

Waveform data have been collected from voluntary participants in the Post Intensive Care Risk Alerting and Monitoring (PICRAM) - II trial. This waveform data was collected using continuous monitoring equipment provided by Hidalgo Ltd. with an attached transmittance photoplethysmograph sensor provided by Nonin Medical Inc. The data was collected at both the John Radcliffe and the Reading Berkshire hospital. In this research only the data collected at Oxford John Radcliffe has been used for analysis.

Time-stamped observations for patients admitted to the ward at the John Radcilffe hospital are recorded within the experiment. The data corresponds to admissions between 2013 and 2014. Sampling frequencies were 256 Hz for the electrocardiogram (ECG), 75 Hz for the PPG, and 25 Hz for the accelerometer. The wearable sensors are shown on a mock patient in Fig. 1. In the following, the methods for estimation of RR from PPG and accelerometer have been explained.

Ten patients (five male, five female) were selected from a larger dataset. These selected patients' age range was from 45 to 77 years old at the time of discharge from the ICU. The select patients' mean age was calculated as 63.7 years old. The length of their stay at the ICU ranged from 1 day to 15 days. The hospital length of stay for these patients ranged from 7 days to 47 days. All patients were white except one with black/British black ethnicity.

B. PPG-Based Respiratory Rate Estimation

1) Signal Quality Index: To evaluate the quality of the PPG signal for estimation of RR, a designed signal quality index (SQI) has been used in the pre-processing stage. The SQI index has been obtained by considering the agreement between two independent peak-detector algorithms [19]. The SQI range is [0 1] where 0 represent the lowest quality and 1 represent the highest quality of the data. The SQI has been used and validated in various research studies especially for reliable estimation of average heart rate. In this research, SQI algorithm has been applied to PPG signal segments and a threshold of 0.85 has been employed to consider only those segments with a SQI of equal to or greater than 0.85. It has been observed that this way of PPG segment selection based on an SQI significantly eliminates unreliable respiratory rate estimates which may result from invalid sensor data or highly corrupted signal by various motion interferences. A separately designed respiratory quality index (RQI), which is currently

under further development [20], will be more effective to directly find those segments of PPG signals where reliable RR estimates could be produced.

2) Auto-Regressive Model: After selection of PPG segments with acceptable SQI, two different respiratory-induced modulations [12], [14] are extracted from the PPG signals to estimate respiratory components. These modulations include respiratory-induced intensity variation (RIIV) and respiratory-induced amplitude variation (RIAV). To derive RIIV, a time-series from the peak amplitudes of the PPG signals is constructed. It has been established that the variation in peak amplitudes of the PPG signals is related to variation in intrathoracic pressure leading to a change in the baseline of perfusion [12], [21]. For RIAV, peaks and troughs of the PPG signal have been considered. To derive RIAV, a time-series using the difference between consecutive peak and trough, representing the height of the PPG pulse, has been calculated. This modulation has been believed to be produced as a result of changes in cardiac output related to the quantity of refill in the vessels at the periphery [12], [21]. The other modulation used in previous studies is respiratory-induced frequency variation. This modulation has not been considered in this research. For the continuous PPG recorded in the clinical environment, derivation of reliable RR estimation from this modulation needs more pre-processing of the PPG signals and highly accurately detected pulse peaks and troughs. For example, minor dislocated peaks on the PPG signals have less effect in derivation of the other two modulations but more effect on the frequency modulation, leading into an inaccurate estimated RR. In addition, some patients studied in this research suffered from atrial fibrillation (AF) where the respiratory-induced frequency variations have been shown not to be able to produce valid results. The effect of AF on respiratory-induced frequency variation can be further investigated in future studies.

Once the amplitude and intensity modulation time-series are constructed from PPG signals, the auto-regressive (AR) model with a varying model orders e.g. $p = 1,\ldots,19$ are applied to each modulation. This is introduced in [14], where instead of selecting an optimal model order, the results from different model orders are fused to get an enhanced AR spectrum based on getting a median of AR spectrum for all model orders. From each modulation, based on the median of AR spectral components, the frequency in the range of 0.05 Hz to 1 Hz with maximum peak amplitude can be selected to obtain the RR in terms of breaths per minute (bpm). Then, RR estimates from two modulations must be fused. In this research, a simple comparison of the estimated RR from the two modulations has been performed. Based on this, when the difference between the estimated RR from two modulations is less than or equal to 3bpm, an average of the two estimated RRs has been used as the final estimated RR. Otherwise, the algorithm fails to produce highly reliable RR estimate.

C. Accelerometry-Based Respiratory Rate Estimation

To estimate respiratory rate based on acceleration signals, a low-pass or band-pass filtering should be applied to each axis separately, then, a frequency in the range of 0.05 Hz to 1 Hz with maximum peak amplitude in spectral domain can be selected to calculate the breaths per minute. A number of studies [22]–[25] have investigated the estimation of respiratory rate from acceleration signals. A Gas pressure system has been used to validate estimation of respiratory rate from accelerometers placed on the subject's sternum [26]. The relative mean error of -0.15 bpm has been also reported. In [27], chest worn accelerometers have been used to estimate respiratory rate in addition to derive angular rate of breathing motion verified by gyroscopes providing high correlation to flow rate measurement from a nasal cannula. A single chest patch sensor containing ECG and accelerometers has been used in [28] to compare fusion of three respiratory rate estimates; one estimate from accelerometer, two estimates using ECG from respiratory sinus arrhythmia and QRS modulation, to the capnography derived based reference [28].

For most of these studies basic signal filtering has been applied to estimate RR which could lack generalisation. In this study, adaptive line enhancer (ALE) has been applied to acceleration signals in the pre-processing stage to aid in separation of the narrow-band signal from broad-band noise and also to select an axis producing the highest signal-to-noise-ratio (SNR).

1) Adaptive Line Enhancer: The ALE, introduced in [29], has been used in many applications [30] such as communication systems [31], biomedical engineering [32], [33] and industrial applications [34] for separation of a low-level sinusoid or a narrow-band oscillation from broad-band noise. The core concept of the ALE is based on linear prediction where the nearly-periodic signal is believed to be perfectly predicted based on the past samples while a non-periodic signal cannot be predicted. Therefore, a delayed version of the input signal has been used as a reference signal into the least-mean-square (LMS) adaptive filter and the desired signal has been considered as the original signal. The error signal of the LMS filter is the estimated noise of the input signal and the output signal is the desired separated signal. To estimate RR using acceleration signals, the ALE has been applied to each accelerometer axis separately, where the ratio of the power of signal to the power of noise has been calculated as the SNR. An accelerometer axis with the highest SNR is then selected for further analysis to estimate respiratory rate.

2) Spectral Fusion: After selection of the desired accelerometer axis, fast fourier transform (FFT) can be applied to estimate the highest peak amplitude of the spectrum of ALE signal output in the range of 0.05 Hz to 1 Hz. Then, a frequency with maximum peak amplitude needs to be obtained, however, this frequency does not relate to the respiratory component in all the situations. For some segments of the data, there could be two local maximum peaks in the spectral domain where discrimination of the respiratory frequency is difficult. Using an extensive analysis of acceleration signals, before applying FFT, the singular spectrum analysis (SSA) [35] has been applied to the ALE signal output of the selected accelerometer axis. It has been shown in [36] that after applying SSA into acceleration signals using the resulted eigenvectors and their corresponding eigenvalues, it is

possible to extract the trend of the data or the lowest possible dominant frequency (considering the largest eigenvalues) in the signals.

In this study SSA has been applied to the ALE signal output of the selected accelerometer axis to decompose it into corresponding eigenvectors and eigenvalues [36], [37]. The eigenvectors are sorted in descending order of associated eigenvalues and grouped using a set of indices as {1,2,3} (denoting eigenvectors related to first, second, and third largest eigenvalues) and {2,3} (denoting eigenvectors related to the second and third largest eigenvalues). After grouping the eigenvectors into these two sub-bands (sub-band1 for {1,2,3} indices and sub-band2 for {2,3} indices), a final elementary matrix should be formed by summation of all elementary matrices in each group. Diagonal averaging has been applied to the final elementary matrix for signal reconstruction and a resulted signal has been formed for each group. Therefore, for each sub-band, one narrowband signal has been constructed which has been exposed to the FFT algorithm to estimate and compare the frequency spectrum for two selected sub-bands.

Then, FFT has been applied to each sub-band reconstructed component and the frequency with maximum peak has been considered as potential respiratory components. Then, for each sub-band, the RR is calculated as breaths per minute. If the absolute difference in estimated RR from these two sub-bands is less than 4 bpm, an average RR has been used as the final estimated RR, otherwise, a reliable RR could not be obtained from the acceleration signals. It may be possible to reduce the threshold of 4 bpm by increasing the frequency resolution. The pseudo-code of the RR estimation method from accelerometer signals is presented in Algorithm 1. The block diagrams of the proposed algorithms for PPG and accelerometer based estimation of RR are shown in Fig. 1.

Algorithm 1: Estimation of RR From Accelerometer

Input accelerations
$a_1(t) \leftarrow$ lateral, $a_2(t) \leftarrow$ vertical, $a_3(t) \leftarrow$ longitudinal
Apply ALE
Set δ, M, N, mu, $L = \text{length}(\mathbf{a})$, $i = 1, 2, 3$
$[\widehat{a}_i(t), \widehat{e}_i(t)] \leftarrow \text{NLMS}(a_i(1:L-\delta), a_i(\delta+1:L), M, N, mu)$
Select accelerometer axis
$\text{SNR}_i = log[\frac{P_{\widehat{a}_i(t)}}{P_{\widehat{e}_i(t)}}]$
$index = max_i(\text{SNR}_i)$
Apply SSA
$\mathbf{X} \leftarrow$ trajectory-matrix $[\widehat{a}_{index}(t)]$
$[\mathbf{U}, \Lambda, \mathbf{V}] \leftarrow$ Apply SVD onto $\mathbf{X}$
$\widehat{\mathbf{X}}_1 = \sum_{j=1,2,3}[\sqrt{\lambda_j}\mathbf{u}_j\mathbf{v}_j^T]$, sub-band1
$\widehat{\mathbf{X}}_2 = \sum_{j=2,3}[\sqrt{\lambda_j}\mathbf{u}_j\mathbf{v}_j^T]$, sub-band2
$[\mathbf{s}_1, \mathbf{s}_2] = \text{diagonal-averaging}(\widehat{\mathbf{X}}_1, \widehat{\mathbf{X}}_2)$
Apply FFT
$f1 = \text{fft}(\mathbf{s}_1)$, $f2 = \text{fft}(\mathbf{s}_2)$
Estimate RR for each sub-band
Find max spectral peaks of $(f1, f2)$: range [0.08Hz-1Hz]
Calculate $[r_1, r_2]$ in terms of bpm
Output RR as mean of $[r_1, r_2]$ if $|\text{diff}(r_1, r_2)| < 4$ *bpm*

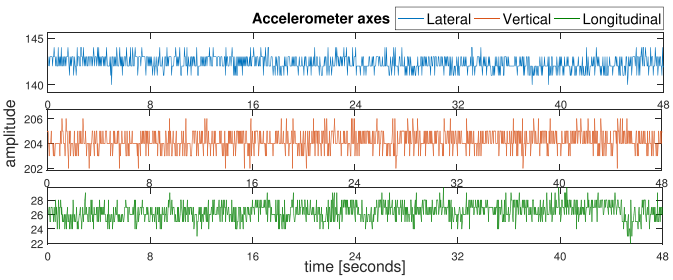

Fig. 2. Raw acceleration signals from three axes for patient #27. The used accelerometer axes are lateral, vertical, and longitudinal.

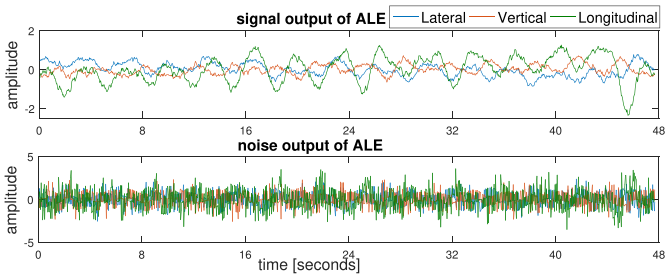

Fig. 3. The signal and noise components of the accelerometer axes are separated by applying ALE. The estimated signal and noise output of the ALE for three accelerometer axes are shown in the *top row* and *bottom row* respectively.

III. Results

A. RR Estimation Using PPG

For estimation of RR from PPG signals, as explained in the previous section, first the SQI is estimated for segmented PPG signal. The windowed segments of 32-seconds with no overlap have been used to estimate SQI. Those PPG segments with calculated SQI of equal or more than 0.85, are used for further analysis to estimate RR. In the next stage, the amplitude and intensity modulation time-series [14] are generated. For each generated time-series, the AR spectrum with model orders of p = 2…18 are constructed. A median AR spectrum has been constructed for each modulation. Then the maximum peak in the AR spectrum has been picked out to be a candidate as the respiratory component. RR has been calculated for each modulation. If there is a difference of less than or equal to 3 bpm, an average RR has been recorded for the corresponding segment. Otherwise, a highly reliable RR estimate has not been found. In the following, RR is estimated from acceleration signals and the results are compared.

B. RR Estimation Using Accelerometer

For estimation of RR from accelerometer signals, the ALE has been applied to each axis of the accelerometer signal to separate the oscillatory and noise component of the axes. As one example, the raw acceleration signals for a selected subject (#27) are shown in Fig. 2. After applying ALE to these segments, the output signal component of all three axes are shown in Fig. 3. A delay (δ) of 10 samples has been used to generate the reference signal for the adaptive filter. The normalised least mean square (NLMS) adaptive filter

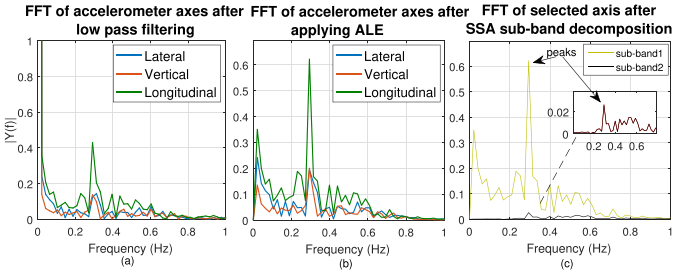

Fig. 4. (a) FFT applied to accelerometer axes after performing low-pass filtering is compared to the results of (b) FFT applied to the signal output of ALE. In (c) sub-band decomposition shows two maximum peaks to be in agreement to represent a respiratory rate component. The estimated respiratory rate has been obtained as 17.62 pbm at Jun.06.2013 14:03:23. The closest manual observation has been recored as 19 bpm at Jun.06.2013 13:50:00.

with an order of ($M = 20$), and an offset of ($N = 50$) has been applied. The acceleration segments are segmented into 64-seconds windowed data segments. However, the first 16 seconds have been discarded and windows of 48-seconds long have been used to estimate RR. A reduced window size of 48-seconds warrants convergence of the NLMS and also is less than two times of the window size used in the PPG-based analysis (32-seconds). As it can be seen from Fig. 3, the noise and signal component of each accelerometer axis are separated.

The SNR as the power of signal to the power of noise has been calculated as 0.19, 0.11 and 0.32 for axis 1 (lateral), 2 (vertical), and 3 (longitudinal) respectively. The highest SNR corresponds to axis 3 (longitudinal axis). This axis has been selected for further analysis to estimate RR. In Fig. 4, the accelerometer axes are compared in spectral domain using FFT. As it can be seen from Fig. 4, FFT applied to the low-pass filtered accelerations shows similar maximum peak (considering frequencies more than 0.1Hz) for all the axes. Although FFT applied to each ALE output shows an enhanced spectrum. The selected accelerometer axis with the largest SNR (third axis for this segment) has been subjected to the spectral sub-band decomposition procedure using SSA. This procedure is necessary for proper analysis of acceleration signals. Sometimes, a sharp change of amplitudes in the acceleration signal creates a low frequency in the spectral domain which is not related to the respiratory component.

Therefore, SSA has been applied to the ALE signal output of the selected accelerometer for sub-band analysis. As explained in the previous section, two new signals are reconstructed in sub-band1 and sub-band2. Then, FFT has been applied to output an estimated RR where the difference of estimated RR in the two specified sub-bands is less than 4bpm.

For patient #27, at Jun.06.2013 13:50:00, a manual observation of RR as 19 bpm was recorded. In the midnight of Jun.07.2013, after about 10 hours and 10 minutes, a manual observation of RR as 22 bpm was recorded. In this time interval, the maximum, minimum and mean recorded RR was obtained as 22 bpm, 18 bpm and 19.92 bpm. The respiratory rate as any other vital can change instantaneously. However, the trends of variations over a long period of time is of clinical importance to detect critical events such as

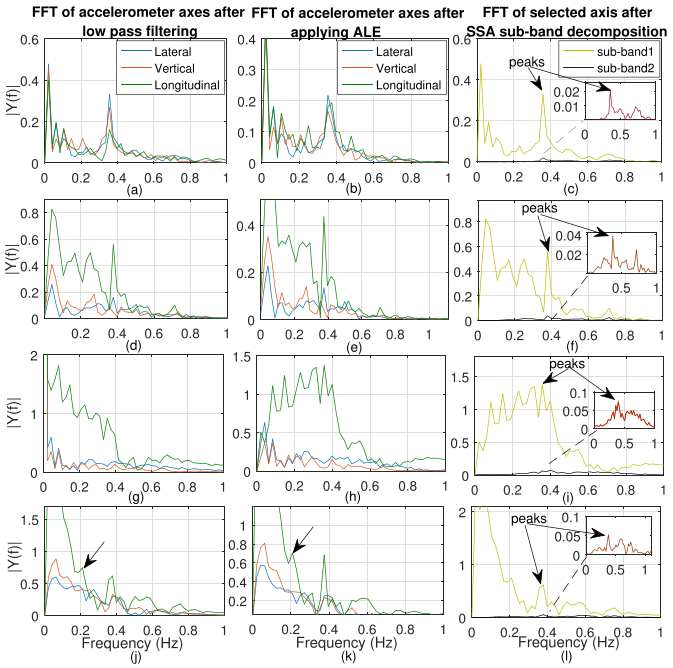

Fig. 5. (a-c) *Example 1:* All three accelerometer axes provide a dominant low frequency peak around frequency of ≈ 0.35Hz (≈ 21 bpm) by applying low pass filtering and ALE which is in a good agreement to manually recorded observation. (d-f) *Example 2:* This example highlights the importance of selection of the best accelerometer axis. (g-i) *Example 3:* This example demonstrates that there is a strong low frequency component which can negatively affect RR estimation. However, the proposed method is able to find valid frequency peaks related to RR. (j-l) *Example 4:* This example shows that a low frequency edge can affect the RR estimation, therefore, sub-band decomposition and comparison using SSA is necessary.

patient deteriorations. The selection of patient #27 is based on low variability of the manual observations to demonstrate cases where applying FFT alone to the accelerometer axes is not effective. In addition, applying SSA sub-band decomposition to select an appropriate frequency band to estimate RR is necessary. A wrongly selected frequency sub-band could lead to major errors of 10 bpm or more in estimation of RR.

In Fig, 4(c), the FFT applied to each sub-band has been shown where the first sub-band related to grouping {1,2,3} eigenvectors has greater peak amplitude comparing to the the second sub-band {2,3}. In both sub-bands the maximum spectral peaks are in close agreement. For this segment of the data, the estimated RR has been obtained as 17.62 pbm at June.06.2013 14:03:23. The closest manual observation has been recored as 19 bpm at June.06.2013 13:50:00. In Fig. 5, four examples from subject #27 are provided to further demonstrate an emphasize on the importance of applying ALE and SSA sub-band decomposition for a reliable estimation of RR.

Example 1: All three accelerometer axes demonstrate a dominant low frequency peak around frequency of ≈ 0.35Hz ($\approx$ 21 bpm) by applying low pass filtering and ALE (Fig. 5(a-c)). The corresponding segmented window for this observation starts at Jun.06.2013 19:30:28 where a manual RR of 22 has been recorded at Jun.06.2013 19:30:00. The estimated RR using the proposed method has been calculated as 21.39 bpm. The maximum spectral peak is in a good agreement to the recorded manual observation.

Example 2: Two accelerometer axes demonstrate dominant spectral peak around frequency of 0.38Hz (22.8 bpm) while the other axis shows a maximum peak around 0.3Hz (15 bpm) (Fig. 5(d-f)). This example shows that selection of the best accelerometer axis is necessary. The ALE is expected to find the best axis using SNR information.

Example 3: This example shows that there is a strong low frequency component which has affected the results after low-pass filtering (Fig. 5(g-i)). This example shows that FFT applied to raw acceleration, produces a maximum peak in frequencies of less than 0.2 Hz (Fig. 5(g) - relating to a respiratory rate of about 12 bpm). A band-pass filter with lower and upper cutoff frequencies as 0.05 Hz and 1 Hz, has also been applied to raw acceleration where the maximum peak happens before 0.2 Hz. However, the output of the ALE has produced SNR of 0.31, 0.17, 1.46 for axis 1 (lateral), 2 (vertical), and 3 (longitudinal) respectively. The FFT applied to the third axis (which has the highest SNR) has produced a spectral peak around 0.4Hz after applying FFT to the signal ALE output (see Fig. 5(h)). The sub-band decomposition of the ALE signal output. of the third axis is shown in Fig. 5(i) where the largest peaks in both sub-bands are in close agreement to produce a reliable RR estimate. The average of these peaks has been used to estimate the final RR. For this segment, the estimated RR has been estimated as 23.91 bpm at Jun.06.2013 19:33:36 where the closest bpm observed manually has been 22 bpm at Jun.06.2013 19:30:00. For this example, only a band-pass filter with cut-off frequencies of [0.2Hz-0.5Hz] could derive the frequency spectrum with a peak around 0.4 Hz while our method is able to find a good match in filtered signals in two sub-bands. However, band-pass filtering with lower cut-off frequency of 0.2Hz (12 bpm) does not have a feasible application for normal/abnormal patients.

Example 4: This example shows that a low frequency edge can produce an uncertainty in the RR estimation (Fig. 5(j-l)). For example, an edge frequency of about $\approx$ 0.2Hz ($\approx$ 12 bpm) will be picked after applying low-pass filtering and also the SSA algorithm - sub-band1 - as the maximal spectral peak, while there is one dominant frequency at $\approx$ 0.38Hz ($\approx$ 22.8 bpm). Based on prior knowledge, investigating manual observations and matching to PPG-based estimates, the frequency of about 0.38 (22.8 bpm) is the actual RR related frequency.

For this example, our method failed to select a peak related to RR since there is not a good match in the frequency domain of the two reconstructed sub-band signals; therefore, there is an uncertainty in the estimation of RR and no RR has been returned by the proposed algorithm. On the other hand, FFT based algorithm outputs an RR of about 12 bpm which is related to a frequency edge and very likely a result of an induced transient motion. Therefore, it is invalid.

Uniform acceleration signals (e.g. Fig. 2 and Fig. 3) are expected to provide clear spectrum. By detailed examination of the raw acceleration signals, it is found that any types of motions, specially transient motion interferences not related to respiration produce low frequency edges or artefacts on the resulted accelerometer spectrum. The spectrum of the two types of these low frequency artefacts are shown in examples 3 and 4. Both examples 3 and 4 demonstrate the sensitivity of the spectral analysis on acceleration signals.

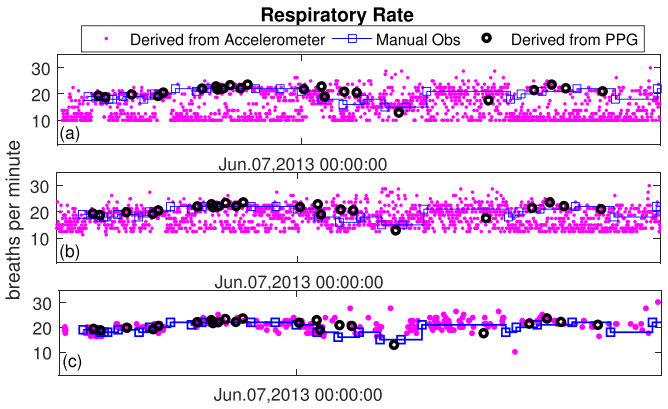

Fig. 6. (a) FFT has been applied to band-pass filtered signal in a range of [0.1Hz-1Hz], (b) FFT has been applied to band-pass filtered signal in a range of [0.2Hz-1Hz], then, RR has been estimated as the maximum spectral peak among all 3 accelerometer axes. (c) The results of proposed technique where only outputs an RR in the case of observing shared low frequency content.

For subject #27, two band pass filters with cut-off frequencies in the range of [0.1Hz-1Hz] and [0.2Hz-1Hz] are applied to all acceleration signals. Then, the maximum spectral peak in the low-frequency range of [0.08Hz-0.5Hz] among all the axes after applying FFT has been used to estimate respiratory rate. The results are provided in Fig. 6(a,b). In addition, our method including ALE and SSA sub-band decomposition has also been applied to the acceleration signals (Fig. 6(c)). It is evident from Fig. 6(a,b), that the estimated RR does vary continuously from 10 to 20. By detailed investigation of accelerations segments, it was obvious that transient motion induced quantities affect the signal spectrum in low frequency domain creating a breathing rate of $\approx$ 10 bpm related to a picked frequency edge. By testing several acceleration segments producing a breathing rate of $\approx$ 10 bpm and slightly reducing or shifting windowed acceleration segments to include only uniform accelerations, the breathing rates of around 20 bpm were re-calculated. This confirmed continuous change of breathing rate from $\approx$ 20 bpm to $\approx$ 10 bpm is mostly invalid.

As Fig. 6(c) demonstrates, our method minimizes the effects low frequency artefacts in respiration derived spectrum by using the SSA method which attempts to find a shared low frequency component in the reconstructed signals of two sub-bands. Although fewer number of RRs could have been obtained using our method, however, good agreements between manual observation, accelerometer and PPG-based estimates for subject #27, highlight the advantages of our method.

C. Respiratory Rate Monitoring of Post-ICU Patients

For the patients selected in this study, the RR has been estimated from accelerometer and PPG signals and they are compared. In addition, manual observations which were recorded by the nurses in an average of every 6 hours are compared to the RR estimations. In Fig. 7, the results of estimated RR

TABLE I
COMPARISON OF PPG AND ACCELEROMETER RR ESTIMATES

	PPG			Accelerometer		Difference
patient ID	segments No. (hours)	segment No. SQI ≥ 0.85	ratio (%) of smart fusion	segments No. (hours)	ratio (%) of spectral fusion	MAE (bpm)
18	1543 (13.72)	1281	20.69	3989 (70.92)	28.48	1.34
16	2403 (21.36)	2018	12.00	1397 (24.84)	12.46	1.81
34	2699 (23.10)	812	23.40	1450 (25.78)	18.00	1.24
43	3121 (27.75)	2930	17.62	3993 (70.99)	12.28	1.56
45	3007 (26.73)	1923	15.61	1540 (27.38)	19.81	1.52
36	502 (4.47)	351	12.54	1488 (26.46)	18.08	1.84
13	1514 (13.46)	946	11.89	3976 (70.69)	6.19	2.56
15	1519 (13.51)	200	22.00	3925 (69.78)	9.69	0.90
23	533 (4.74)	404	10.15	1375 (24.45)	25.10	1.73
27	637 (5.67)	507	5.13	1655 (29.43)	16.02	1.86

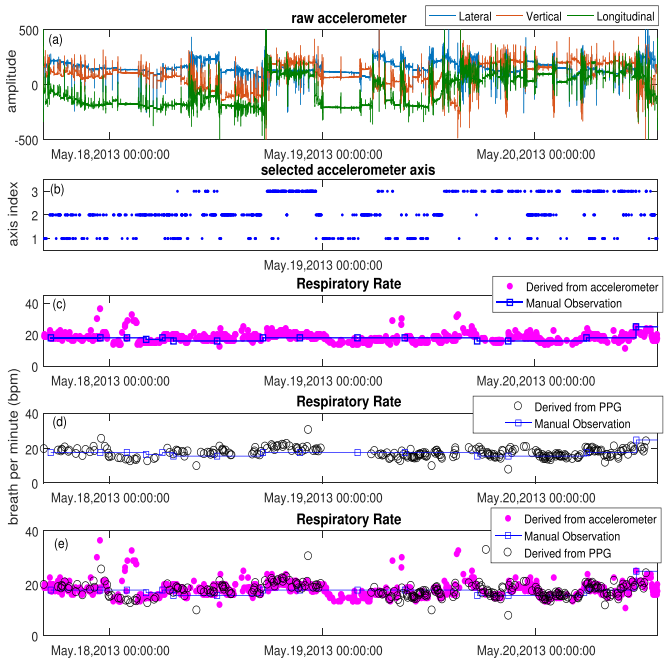

Fig. 7. (a) Raw acceleration signals recorded for more than 2 days for patient #18. (b) Selected accelerometer axis after applying adaptive line enhancer based on SNR (axis 1, axis 2 and axis 3 denote lateral, vertical and longitudinal axis respectively). (c) Estimated respiratory rate from accelerations. (d) Estimated RR from PPG signal. (e) Respiratory rate obtained in (c-d). In plots (c-d), recorded manual observation are shown as blue squares.

from acceleometer and PPG signals are shown for subject #18. This subject shows continuous recorded signals for more than 2 days. In Fig. 7(a), the raw accelerations are shown. The selected accelerometer axis are indexed in Fig. 7(b) where axis 1, 2 and 3 denote lateral, vertical and longitudinal axes. The accelerometry based estimation of RR has been plotted in Fig. 7(c) while the

PPG-based estimation of RR has been plotted in Fig. 7(d). These two estimations using the timestamps are overlapped and plotted in Fig. 7(e) which demonstrate a strong agreement between RR estimates for most parts of the recorded signals. As it can be seen from Figure 7, there are more RR estimates from accelerometer than PPG-based estimates.

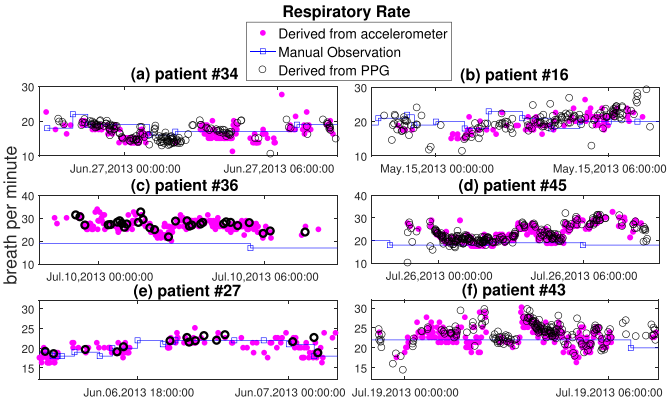

Fig. 8. For six selected patients, the RR estimated from accelerometer and PPG signals in segments of more than 6 hours versus recorded manual observations are shown.

For a subset of 6 selected patients, the PPG and accelerometer based estimates are shown in Fig. 8. These segments of the data relate to segments of more than 6 hours long. In both Figs. 7 and 8, the manual observations are denoted as blue squares. It can be seen that there are cases where the manual observation does not agree with both PPG and accelerometer based estimates while there is a good agreement between PPG and accelerometer-based estimates. The results of comparable RR estimates from PPG and accelerometer based on the matching time-stamps are shown in Fig. 9.

In Table I, for 10 selected patients, detailed statistics are provided. Based on this table, the number of PPG segments to estimate RR is shown in the second column for each subject. These segments are converted to their time duration in terms of the number of hours of recorded PPG data. Then, the number of segments with SQI of greater than or equal to 0.85 is provided in the third column. The percentage of segments produced RR estimates based on smart fusion (agreement of AR spectrum in two modulations) are shown for each subject. For accelerometer based estimation of RR, the initial number of segments and the corresponding time duration in terms of the hours of data are provided. Also the percentage of obtained segments to estimate RR based on spectral fusion (agreement in two sub-bands) is provided.

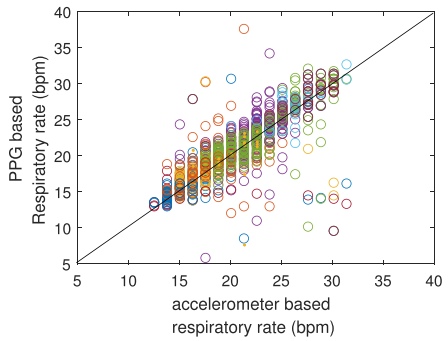

Fig. 9. Accelerometer (25Hz)-based RR estimates versus PPG (75Hz)-based estimates.

The time-stamps have been used to compare the errors of pairwise estimated RRs where both PPG and accelerometer-based RR estimates are available. The mean absolute error (MAE) is shown in the last column of Table I. As it can be seen from Table I, all the resulted MAEs are less than 2.60 bpm. It should be noted that the sample size to calculate the MAE is not the same for all the subjects. Meanwhile, very good MAEs have been achieved for most subjects (less than 2 bpm). The accelerometers have been able to produce RR estimates for about 70 hours of the continuous data while this has been recorded for about 27 hours of PPG data. Although after data fusion, for error measurements, the number of segments are reduced to consider highly reliable RR outputs of the algorithms.

IV. Discussion

There is an essential need for having a mobile and portable respiration system to continuously monitor patients in critical conditions, following vital events or post operation. Respiratory rate has been focused to be estimated from PPG and ECG signals in recent years. However, RR estimation from accelerometer as a motion-based sensor has been extremely limited in research studies. In addition, continuous monitoring of RR in a clinical environment for few hours/days has not been studied from real data collected in the hospital which is a unique contribution of this research.

In this research, accelerometers have been studied for estimation of RR for monitoring patients following discharge from ICUs. The results of estimated respiratory rate from two different signal modalities (PPG and accelerations) in a continuous long period of time have shown to be in close agreement for many segments across patients. The wearable sensor signals used in clinical environments could be severely affected by various motion interferences, sensor fault, and detachment. Both PPG and accelerometer based algorithms impose constraints to select high quality segments of the data and output only reliable respiratory rate estimates. Arm-worn acceleration signals have shown a big potential to be used for estimation of RR for both static and mobile patients.

In the current study, fewer RR parameters were produced using PPG signal input comparing to the use of acceleration signals. This is a consequence of applying SQI related algorithm to the data before applying the RR algorithm. In addition, smart fusion of RR estimation from two different modulations has produced one final RR estimate only where there are close estimated RRs from both modulations. Otherwise, the algorithm has not been able to output a reliable RR estimate. The comparison of RRs has been performed when both PPG and accelerometry based algorithms have been able to output reliable RR values. In future studies, the PPG-based respiratory rate estimation algorithm could be applied to the continuous recorded PPG signals from wrist/finger worn sensors in the clinical setting to provide reliable RR estimates based on designing a new RQI.

Accelerometry-based analysis of RR can be further improved and validated using both PPG and ECG signals in future studies. The spectral fusion performed in this study based on the output of the ALE and applying SSA algorithm has shown to be effective in producing more reliable RR estimates. This spectral fusion stage can be further improved in future studies to produce as many as RR estimates which are highly reliable across consecutive segments and various patients. In addition, activity classification from acceleration signals can be performed using accelerometer information from other sources such as mobile phone. Joint activity classification and estimation of respiratory rate from arm/chest worn sensor can be studied in succeeding studies. Moreover, fusion of RR estimation from various sensors that could be accelerometers on different positions, and also from combination of PPG and accelerometer can improve the results. This research has also provided a big motivation to use accelerometers for small validation studies versus invasive ground truth data where different body positions (such as arm and chest) and also vary sampling frequencies of accelerometers to observe related performance. Mobile phones can also be placed on the chest and used for certain patient groups to evaluate the estimation of RR from their integrated accelerometer unit. Comparison of arm and chest worn accelerometers for RR monitoring can be performed in the future studies where highly reliable ground truth reference data is required to make accurate inference.

Acknowledgment

The authors would like to thank Marco Pimentel for help on analysis of PPG-based estimation of respiratory rate.

References

[1] P. B. Lovett, M. J. Buchwald, K. Stürmann, and P. Bijur, "The vexatious vital: Neither clinical measurements by nurses nor an electronic monitor provides accurate measurements of respiratory rate in triage," *Ann. Emergency Med.*, vol. 45, pp. 68–76, Jan. 2005.

[2] R. F. T. Yilmaz and Y. Hao, "Detecting vital signs with wearable wireless sensors," *Sensors*, vol. 10, no. 12, pp. 10837–10862, 2010.

[3] B. G. Goudra, L. C. Penugonda, R. M. Speck, and A. C. Sinha, "Comparison of acoustic respiration rate, impedance pneumography and capnometry monitors for respiration rate accuracy and apnea detection during GI endoscopy anesthesia," *Open J. Anesthesiol.*, vol. 3, pp. 74–79, Jul. 2013.

[4] M. Młyńczak and G. Cybulski, "Impedance pneumography: Is it possible?" *Proc. SPIE*, vol. 8454, p. 84541T, Oct. 2012.

[5] L. Tarassenko, D. A. Clifton, M. R. Pinsky, M. T. Hravnak, J. R. Woods, and P. J. Watkinson, "Centile-based early warning scores derived from statistical distributions of vital signs," *Resuscitation*, vol. 82, no. 8, pp. 1013–1018, 2011.

[6] D. Sbiti-Rohr *et al.*, "The national early warning score (NEWS) for outcome prediction in emergency department patients with community-acquired pneumonia: Results from a 6-year prospective cohort study," *BMJ Open*, vol. 6, no. 9, p. e011021, 2016.
[7] T. J. Hodgetts, G. Kenward, I. G. Vlachonikolis, S. Payne, and N. Castle, "The identification of risk factors for cardiac arrest and formulation of activation criteria to alert a medical emergency team," *Resuscitation*, vol. 54, pp. 125–131, Aug. 2002.
[8] C. Subbe, R. G. Davies, E. Williams, P. Rutherford, and L. Gemmell, "Effect of introducing the modified early warning score on clinical outcomes, cardio-pulmonary arrests and intensive care utilisation in acute medical admissions," *Anaesthesia*, vol. 58, pp. 797–802, Aug. 2003.
[9] S. Ridley, "The recognition and early management of critical illness," *Ann. Roy. College Surgeons England*, vol. 87, no. 5, pp. 315–322, 2005.
[10] M. H. Ebell, "Predicting pneumonia in adults with respiratory illness," *Amer. Family Phys.*, vol. 76, no. 4, pp. 560–562, 2007.
[11] M. A. Cretikos, R. Bellomo, K. Hillman, J. Chen, S. Finfer, and A. Flabouris, "Respiratory rate: The neglected vital sign," *Med. J. Austral.*, vol. 188, p. 657, Jan. 2008.
[12] W. Karlen, S. Raman, J. M. Ansermino, and G. A. Dumont, "Multiparameter respiratory rate estimation from the photoplethysmogram," *IEEE Trans. Biomed. Eng.*, vol. 60, no. 7, pp. 1946–1953, Jul. 2013.
[13] P. H. Charlton, T. Bonnici, L. Tarassenko, D. A. Clifton, R. Beale, and P. J. Watkinson, "An assessment of algorithms to estimate respiratory rate from the electrocardiogram and photoplethysmogram," *Physiol. Meas.*, vol. 37, no. 4, p. 610, 2016.
[14] M. A. F. Pimentel *et al.*, "Toward a robust estimation of respiratory rate from pulse oximeters," *IEEE Trans. Biomed. Eng.*, vol. 64, no. 8, pp. 1914–1923, Aug. 2017.
[15] P. Charlton *et al.*, "Breathing rate estimation from the electrocardiogram and photoplethysmogram: A review," *IEEE Rev. Biomed. Eng.*, to be published, doi: 10.1109/RBME.2017.2763681.2017.
[16] A. Procházka, H. Charvátová, O. Vyšata , J. Kopal, and J. Chambers, "Breathing analysis using thermal and depth imaging camera video records," *Sensors*, vol. 17, no. 6, p. 1408, 2017.
[17] F. Erden, A. Z. Alkar, and A. E. Cetin, "Contact-free measurement of respiratory rate using infrared and vibration sensors," *Infr. Phys. Technol.*, vol. 73, pp. 88–94, Nov. 2015.
[18] J. Jorge *et al.*, "Non-contact monitoring of respiration in the neonatal intensive care unit," in *Proc. IEEE 12th Int. Conf. Autom. Face Gesture Recognit.*, 2017, pp. 286–293.
[19] M. A. F. Pimentel, M. D. Santos, D. B. Springer, and G. D. Clifford, "Heart beat detection in multimodal physiological data using a hidden semi-Markov model and signal quality indices," *Physiol. Meas.*, vol. 36, pp. 1717–1727, Jul. 2015.
[20] D. A. Birrenkott, M. A. F. Pimentel, P. J. Watkinson, and D. A. Clifton, "Robust estimation of respiratory rate via ECG- and PPG-derived respiratory quality indices," in *Proc. IEEE Annu. Int. Conf. Eng. Med. Biol. Soc.*, Orlando, FL, USA, Aug. 2016, pp. 676–679.
[21] D. J. Meredith, D. Clifton, P. Charlton, J. Brooks, C. W. Pugh, and L. Tarassenko, "Photoplethysmographic derivation of respiratory rate: A review of relevant physiology," *J. Med. Eng. Technol.*, vol. 36, no. 1, pp. 1–7, 2012.
[22] P. Jiang and R. Zhu, "Dual tri-axis accelerometers for monitoring physiological parameters of human body in sleep," in *Proc. IEEE SENSORS*, Nov. 2016, pp. 1–3.
[23] M. Haescher, D. J. C. Matthies, J. Trimpop, and B. Urban, "A study on measuring heart- and respiration-rate via wrist-worn accelerometer-based seismocardiography (SCG) in comparison to commonly applied technologies," in *Proc. 2nd Int. Workshop Sensor-Based Activity Recognit. Interact.*, 2015, Art. no. 2.
[24] D. S. Morillo, J. L. R. Ojeda, L. F. C. Foix, and A. L. Jiménez, "An accelerometer-based device for sleep apnea screening," *IEEE Trans. Inf. Technol. Biomed.*, vol. 14, no. 2, pp. 491–499, Mar. 2010.
[25] Z. Zhang and G.-Z. Yang, "Monitoring cardio-respiratory and posture movements during sleep: What can be achieved by a single motion sensor," in *Proc. IEEE 12th Int. Conf. Wearable Implant. Body Sensor Netw. (BSN)*, Jun. 2015, pp. 1–6.
[26] S. P. Preejith, A. Jeelani, P. Maniyar, J. Joseph, and M. Sivaprakasam, "Accelerometer based system for continuous respiratory rate monitoring," in *Proc. IEEE Int. Symp. Med. Meas. Appl. (MeMeA)*, May 2017, pp. 171–176.
[27] A. Bates, M. J. Ling, J. Mann, and D. K. Arvind, "Respiratory rate and flow waveform estimation from tri-axial accelerometer data," in *Proc. Int. Conf. Body Sensor Netw.*, Singapore, Jun. 2010, pp. 144–150.
[28] A. M. Chan, N. Ferdosi, and R. Narasimhan, "Ambulatory respiratory rate detection using ECG and a triaxial accelerometer," in *Proc. IEEE Annu. Int. Conf. Eng. Med. Biol. Soc.*, Jul. 2013, pp. 4058–4061.
[29] B. Widrow *et al.*, "Adaptive noise cancelling: Principles and applications," *Proc. IEEE*, vol. 63, no. 12, pp. 1692–1716, Dec. 1975.
[30] R. M. Ramli, A. O. A. Noor, and S. A. Samad, "A review of adaptive line enhancers for noise cancellation," *Austral. J. Basic Appl. Sci.*, vol. 6, no. 6, pp. 337–352, 2012.
[31] J.-D. Wu and S.-L. Lin, "Audio quality improvement of vehicular hands-free communication using variable step-size affine-projection algorithm," *Int. J. Wavelets, Multiresolution Inf. Process.*, vol. 8, no. 6, pp. 875–894, 2010.
[32] D. Jarchi, B. Makkiabadi, and S. Sanei, "Mental fatigue analysis by measuring synchronization of brain rhythms incorporating enhanced empirical mode decomposition," in *Proc. 2nd Int. Workshop Cognit. Inf. Process.*, Jun. 2010, pp. 423–427.
[33] S. Sanei, *Adaptive Processing of Brain Signals*. Hoboken, NJ, USA: Wiley, 2013.
[34] W. Hernández, "Improving the response of a wheel speed sensor using an adaptive line enhancer," *Measurement*, vol. 33, no. 3, pp. 229–240, 2003.
[35] N. G. V. Nekrutkin and A. A. Zhigljavsky, *Analysis of Time Series Structure: SSA and Related Techniques*. Boca Raton, FL, USA: CRC Press, 2001.
[36] D. Jarchi, C. Wong, R. M. Kwasnicki, B. H. G. A. Tew, and G.-Z. Yang, "Gait parameter estimation from a miniaturized ear-worn sensor using singular spectrum analysis and longest common subsequence," *IEEE Trans. Biomed. Eng.*, vol. 61, no. 4, pp. 1261–1273, Apr. 2014.
[37] D. Jarchi, B. Lo, C. Wong, E. Ieong, D. Nathwani, and G.-Z. Yang, "Gait analysis from a single ear-worn sensor: Reliability and clinical evaluation for orthopaedic patients," *IEEE Trans. Neural Syst. Rehabil. Eng.*, vol. 24, no. 8, pp. 882–892, Aug. 2016.

Delaram Jarchi, photograph and biography not available at the time of publication.

Sarah J. Rodgers, photograph and biography not available at the time of publication.

Lionel Tarassenko, photograph and biography not available at the time of publication.

David A. Clifton, photograph and biography not available at the time of publication.